Journal of Membrane Science 523 (2017) 317–326

Contents lists available at ScienceDirect

Journal of Membrane Science

journal homepage: www.elsevier.com/locate/memsci

Preparation, characterization, and applications of electrospun ultrafine fibrous PTFE porous membranes

Yan Huang, Qing-Lin Huang*, Huan Liu, Chao-Xin Zhang, Yan-Wei You, Na-Na Li, Chang-Fa Xiao

State Key Laboratory of Separation Membranes and Membrane Processes, Department of Material Science and Engineering, Tianjin Polytechnic University, Tianjin 300387, China

ARTICLE INFO

Keywords:
Poly(tetrafluoroethylene) (PTFE)
Electrospinning
Ultrafine fiber
Super-hydrophobicity
Membrane distillation (MD)

ABSTRACT

Ultrafine fibrous poly(tetrafluoroethylene) (PTFE) porous membranes (UFPPMs) were prepared by sintering electrospun PTFE/poly(vinylalcohol) (PVA) composite membranes. Meanwhile, poly(acrylonitrile) (PAN) nanofibers were co-electrospun to reinforcing the material. The effects of changing the PTFE/PVA mass ratio, the sintering temperature and the heating rate on the structure and properties of the resulting membranes were investigated. To observe the structure evolution of the ultrafine fibers during the sintering process, the prepared UFPPMs were characterized by scanning electron microscopy (SEM), atomic force microscopy (AFM) and static water contact angles (WCA). A unique interconnected fibrous network structure was formed. The spinning and sintering conditions were optimized. Moreover, the UFPPMs exhibited a super-hydrophobicity and an excellent lipophilicity. They also performed well in harsh water (saline feed solution 3.5 wt% NaCl and 10 wt% NaOH) membrane distillation experiments. The permeate flux stabilized at 14.53 L m^{-2} h^{-1} and the salt rejection remained above 99.8% after operating for 35 h.

1. Introduction

Ultra-fine or nanoscale fibrous, porous membranes are useful materials that have been used in applications such as filtration engineering, drug delivery, electronics, optics, and wound healing [1]. The development of efficient filtration technologies is especially important as water shortages have become a growing global problem in recent years [2]. Membranes are an energy-efficient and environmentally-friendly method to recycle waste water for reuse. However, the fabrication of membranes can be challenging [3]. Electrospinning has emerged as an attractive and simple method for the preparation of nanometer or submicrometer fibrous materials [4,5]. Meanwhile, electrospun nanofiber membranes (ENMs) have shown great potential for use in membrane distillation (MD) because of their high porosity, high flux rates, narrow pore size distribution, and interconnected open structure [6].

Poly(tetrafluoroethylene) (PTFE) has many unique characteristics that include outstanding thermal and chemical stability, high hydrophobicity, high fracture toughness, and low surface friction [7,8]. These exceptional properties make PTFE an ideal membrane material for MD, especially for harsh water that is acidic/alkaline, has high toxin concentrations, or must be filtered at high temperatures. However, PTFE nanofiber or ultrafine fibrous membranes are challenging to fabricate because they are difficult to melt and are largely insoluble in solution. Presently, the commercial preparation of PTFE porous flat-sheet membranes or hollow fiber membranes includes multiple steps such as a lubricated paste extrusion followed by stretching and/or sintering. This process is not only tedious but also leads to materials with poor performance stability owing to the creeping deformation of PTFE [9].

There have been few reports that fabricate PTFE membranes by electrospinning and even fewer reports that have studied the effects of using PTFE on the resulting nanofiber membrane. For example, Guo et al. [10] have fabricated ultrafine PTFE fibers by sintering previously electrospun PTFE/poly(vinyl alcohol) (PVA) fiber. Xiong et al. [11] have also prepared ultrafine PTFE fibrous membranes by sintering previously electrospun PTFE/PVA nanofiber membranes with different PTFE/PVA mass ratios. However, the application of these electrospun ultrafine PTFE fibrous membranes has not been extensively studied.

The goal of this study was to fabricate a super-hydrophobic nanofibrous membrane with high water flux for use in membrane distillation. We explored the effects of the PTFE/PVA mass ratio and the sintering temperature on the structure and properties of ultrafine fibrous PTFE porous membranes (UFPPMs). The performance of the

* Correspondence to: No. 399 West Binshui Road, Xi Qing District, Tianjin Polytechnic University, 300387 Tianjin, China.
E-mail address: huangqinglin@tjpu.edu.cn (Q.-L. Huang).

http://dx.doi.org/10.1016/j.memsci.2016.10.019
Received 13 April 2016; Received in revised form 16 August 2016; Accepted 11 October 2016
Available online 13 October 2016
0376-7388/

UFPPMs was then tested in vacuum membrane distillation (VMD) for the separation of oil and water, and in a harsh water desalination using an alkaline solution.

2. Experimental

2.1. Materials

An aqueous dispersion of PTFE (FR301B) was purchased from 3F New Materials Co., Ltd. Shanghai. The specifications of the dispersion are shown in Table 1. Poly(vinyl alcohol) (PVA, Type1788, degree of polymerization 1700, and degree of alcoholysis 88%) was purchased from Lanbo Industrial Co., Ltd., Hangzhou. Poly(acrylonitrile) (PAN, degree of polymerization 50,000) was purchased from Qilu Petrochemical Technology Co., Ltd. All the reagents were used as received without further purification.

2.2. Membrane preparation

A 10 wt% aqueous solution of PVA was prepared by dissolving PVA powder in distilled water under constant agitation at 80 °C for at least 6 h. The solution was then brought to room temperature and an aqueous dispersion of PTFE was added to the PVA solution with constant stirring for 3 h to form the spinning solutions. PAN was dissolved in N,N-dimethylformamide (DMF) to make a 10 wt% solution.

A schematic diagram of the electrospinning process is shown in Fig. 1. The set-up consists of a syringe feeder system, a metallic ground fiber collector, and a high-voltage power supply which were all housed in a temperature-controlled room. As shown in the schematic (Fig. 1), a three-needles electrospinning setup with linear arrangement was used. The injection syringe containing PAN solution was placed in the middle position, the other two injection syringes containing PVA/PTFE solution were symmetrically distributed on both sides. The syringe was fashioned with a 0.34 mm inner diameter needle by a Teflon tube.

Table 1
Characteristics of the aqueous dispersion of PTFE.

Solid Content	60 wt%
Nonionic Surfactant Content	5 wt%
Average Particle Size	0.19 μm
Viscosity	25×10^{-3} Pa·s
Density	2.20 g/cm^3
pH	9

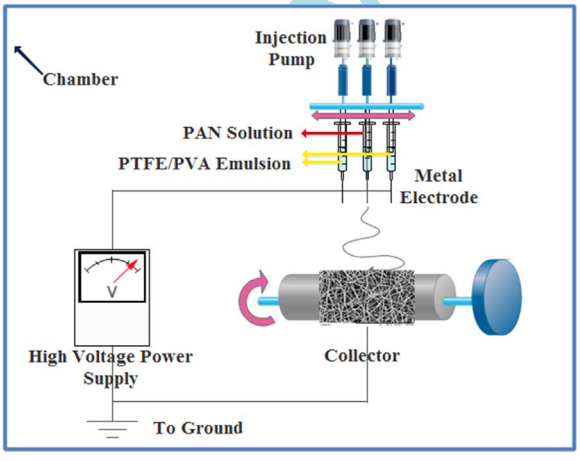

Fig. 1. A schematic diagram of the electrospinning apparatus for manufacturing UFPPMs.

A high electric field was generated between the polymer drop from the needle tip and the fiber collector. The relative humidity and temperature were measured by a hygrothermograph placed inside the electrospinning chamber. They were fixed at values of 70 ± 5% and 25 ± 3 °C, respectively. All solutions (including PAN) were electrospun at an applied voltage of 25 kV, a spinning distance of 10 cm and a fluid flow rate of 0.008 ml/min. As each solvent drop evaporated, the solid polymer fibers began collecting on the electrically-grounded target.

Co-electrospun PAN nanofibers were utilized as reinforcement for the membranes. As for precursor composite PTFE/PVA nanofiber membrane, the mechanical strength and support performance was weak. So, the co-electrospun PAN nanofibers were introduced as reinforcement of the precursor composite membrane because of their good mechanical strength and support performance.

To ensure that all solvents were completely removed, the electrospun PTFE/PVA composite membranes were subsequently placed in a vacuum oven at 60 °C overnight. The dry composite membranes were then sintered in a muffle furnace at 340 °C, 360 °C, 380 °C, or 400 °C to obtain the different membranes. These precursor membranes were named M-p2, M-p4, M-p6, M-p8, and M-p10 according to the different PTFE/PVA mass ratio used (i.e. 2:1, 4:1, 6:1, 8:1, 10:1 wt%: wt%, respectively). After sintering, the sintered membranes were denoted as M-s2, M-s4, M-s6, M-s8, and M-s10. The sintering process fully removed PVA and fused the remaining PTFE resins to form UFPPMs.

2.3. Membrane characterization

2.3.1. Membrane morphologies

The morphologies of the membrane samples were investigated by scanning electron microscopy (FESEM S4800, Hitachi, Japan; SEM TM3030, Hitachi, Japan) after coating with gold and by atomic force microscopy (AFM, CSPM 5500, Benyuan-nano, China). A Hitachi S4800 scanning electron microscope equipped with an energy dispersive X-ray (EDX) spectrometer was used. The diameter distribution of the ultrafine fibers was calculated form the SEM images using Image Proplus software.

2.3.2. Thermogravimetric analysis(TGA)

The thermal degradation behavior of each membrane sample was determined using a thermogravimetric analysis instrument (TA- SDT Q600) under air and at a heating rate of 5 °C/min from room temperature to 800 °C. The membrane sample weights were between 6 and 10 mg.

2.3.3. Contact angle

Contact angle measurements were performed using an optical contact angle meter (modelDSA100, KRUSS Co., Germany) by the sessile drop method of water and oil drops. The measurements were conducted room temperature (25 °C) and at a relative humidity of 40–50%. A droplet of water or oil with a volume of 2 μl was deposited onto the membrane surface from a distance of 5 cm by vibrating the tip of a micro-syringe. The droplet was left on the membrane surface for 60 s before recording. A lens and a source light were used to collect images of the drop and the shape of the drop was analyzed to determine the static contact angle. Five different spots were measured for each sample and the average value of the static contact angles was reported.

2.3.4. Membrane porosity and pore size distribution

The porosity of each membrane was determined by the gravimetric method [12], which is determined from the weight of liquid contained in the membrane pores. Due to the hydrophobicity of PTFE, n-butyl alcohol was used as a wetting liquid. The porosity (ε) of the membrane was determined from Eq. (1)

$$\varepsilon(\%) = \frac{w_2 - w_1}{A \times d \times \rho} \times 100 \quad (1)$$

where w_2 is the weight of the membrane wetted by n-butyl alcohol (g), w_1 is the weight of the dry membrane (g), d is the average thickness of the membrane (cm), ρ is the density of n-butyl alcohol (ρ=0.811 g/ml), and A is the area of the PTFE polymer (cm^2).

The pore size and its distribution of each membrane was determined by the gas permeation method using a capillary flow porometer (CFP-1100-A, Porous Materials Inc., Ithaca, NY). To fully wet the membranes, they were incubated with the wetting liquid for about 24 h. The pore size distribution was determined using computer software coupled to the capillary flow porometer.

2.3.5. Mechanical strength

The tensile strengths of the membranes were determined at room temperature using a JBDL-200N electronic tensile tester (Yangzhou, China) at a tensile rate of 2 mm/min. The membranes were cut into 0.5×5 cm (wide×length) strips, and each specimen was tested five times.

2.3.6. Liquid entry pressure (LEP)

The LEPs of the dried UFPPMs were determined using a laboratory device at room temperature described in literature [13,14], as shown in Fig. 2. The average value of three tests is reported.

2.3.7. Membrane distillation experiments

The performance of the membranes in harsh water desalination was tested with vacuum membrane distillation (VMD), as shown in Fig. 3. The experimental set-up used it described elsewhere [7,14]. The saline feed solution (3.5 wt% NaCl, 10 wt% NaOH) was pre-heated before it was circulated to one side of the membrane. Cell dimensions and the effective membrane area surface were 75.43 cm^2 and 21.23 cm^2, respectively. Hot saline solution (80 °C feed temperature) was pumped to the feed side of the membrane by a diaphragm pump at a constant flow rate of 1.5 L/min. A vacuum was applied using a vacuum pump to the other side of the membrane. The permeate vapor was condensed and collected as the product. The conductivity of the feed solution and the permeate water was measured by a conductivity meter (ST10C-B, OHAUS), and the concentration was calculated by the linear relationship between the conductivity and concentration, which was described elsewhere [14]. The salt rejection R was calculated by Eq. (2):

$$R = \left(1 - \frac{C_p}{C_f}\right) \times 100\% \quad (2)$$

where C_f and C_p are the concentration of the feed solution and permeate water, respectively.

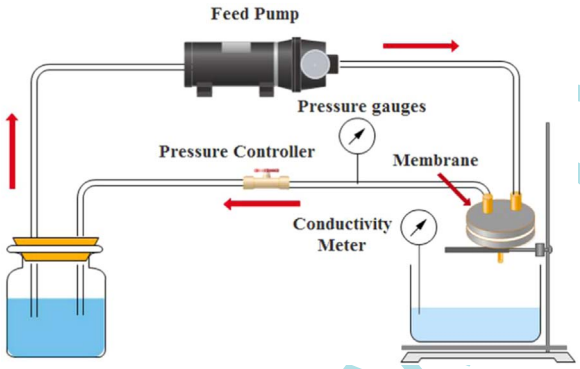

Fig. 2. Testing device for determining the LEP of the UFPPMs.

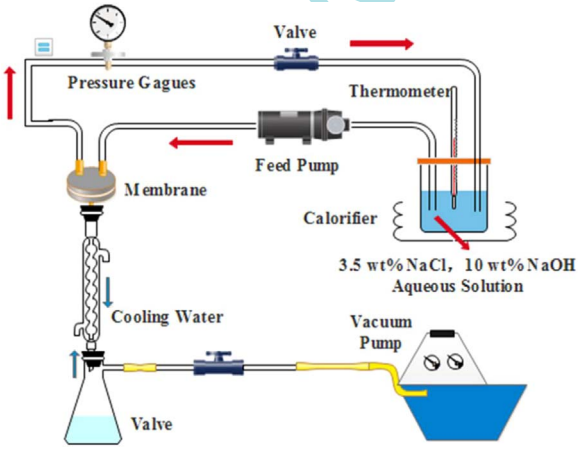

Fig. 3. A schematic diagram of the experimental VMD apparatus.

3. Results and discussion

3.1. Structural analysis

The UFPPMs were produced by sintering the precursor electrospun PTFE/PVA composite membranes in order to decompose the PVA matrix and to bind the remaining PTFE together to form an integrated fibrous network [15,16]. Magnification SEM surface images of UFPPMs were shown in Fig. 4. It could be seen that during the sintering process, PVA were melted and further decomposed; the left PTFE particles gradually fused and further formed an integrated fibrous network; PAN nanofibers formed a stable trapezoidal structure due to the cyclization reaction, which left in the final UFPPMs.

The EDX and the TGA analyses of the UFPPMs, individual components of the PVA, PTFE, and PAN fibers were shown in Fig. 5. It can be seen that, the PVA began to decompose at about 242 °C, the PTFE began to decompose at about 514 °C, and then the PAN fibers began to decompose at about 607 °C. After sintering, the PAN fibers remained in the membranes and continued to play a role in enhancing mechanical strength.

3.2. Membrane morphologies

3.2.1. Effect of PTFE/PVA mass ratios

The surface morphologies of the precursor PTFE/PVA composite membranes at different PTFE/PVA mass ratios are shown in Fig. 6. The electrospinning solution with a PTFE/PVA mass ratio of 2:1 had good spinability and produced electrospun PTFE/PVA fibers with good fibrous structures with PTFE particles wrapped in ultrafine PVA fibers. However, the precursor PTFE/PVA membrane was fragile after sintering (Fig. 6a). When the PTFE content was increased, the PTFE/PVA fibers transformed from fibrous structures to bead-like structures [14]. With a PTFE/PVA mass ratio of 10:1, only bead-like structures were produced. The electrospun PVA fibers could not fully encapsulate whole PTFE particles which led to poor mechanical strength of this PTFE/PVA composite membrane.

The surface morphologies of the UFPPMs (360 °C sintering temperature) prepared from different PTFE/PVA mass ratios, and the diameter distributions of the PTFE ultrafine fibers are shown in Fig. 7. Membranes with a PTFE/PVA mass ratio lower than 6:1 had PTFE ultrafine fiber diameters ranging from about 100–500 nm (Fig. 7a-2-c-2). As the mass ratio of PTFE/PVA increased, the membranes became PTFE resins rather than fibers (Fig. 7c-2-d-2). The surface morphologies of the membranes were also evaluated by AFM. The 3D images are shown in Fig. 7. When the mass ratios of the PTFE/PVA membranes increased from 2:1 to 10:1, the mean roughness (R_a) increased from 123 nm to 317 nm. This explains why the PTFE fibers transformed from a fibrous structure to a bead-like structure at higher mass ratios. High surface roughness has traditionally accompanied a membrane with high hydrophobicity and this was also observed in our

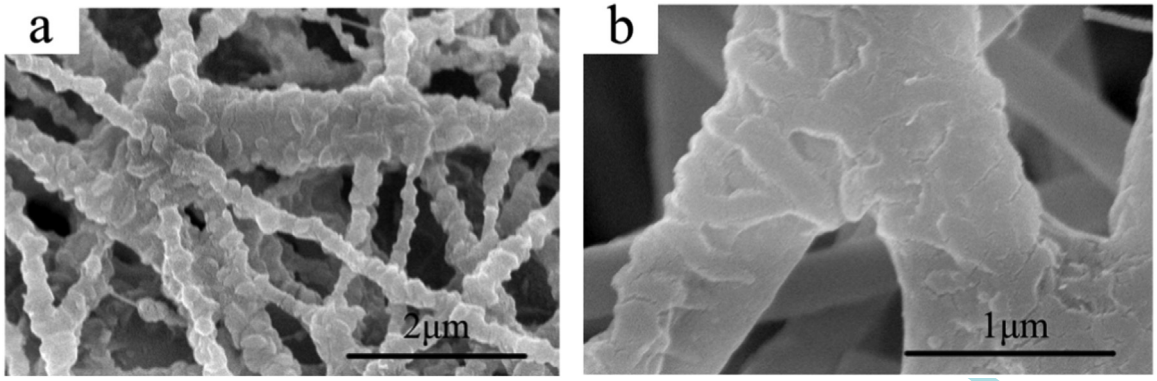

Fig. 4. Morphologies of UFPPMs (M-s6; a:20000×surface, b:40000×surface).

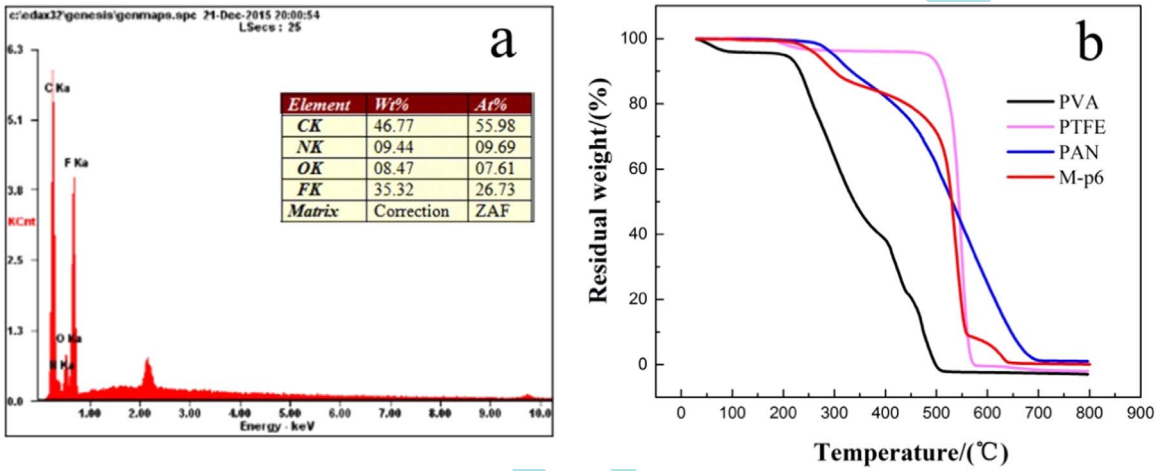

Fig. 5. EDX and TGA analysis of UFPPMs. (a) EDX analysis of M-s6 sintered at 380 °C, (b) TGA analysis of PVA, PTFE, PAN, and M-p6..

case. In this study, a PTFE/PVA mass ratio of 6:1 was chosen for further investigation.

3.2.2. Effects of sintering temperature

In order to obtain UFPPMs with good performances, the sintering treatment was properly optimized [11,17]. When the mass ratio of the PTFE/PVA was 6:1, all of the UFPPMs prepared at different sintering temperatures exhibited an interconnected fibrous network (Fig. 8). Increasing the sintering temperature leads to further melting of the PTFE particles so that the fibers fuse together and the membrane becomes compact. This compacting induces smaller pore size and a higher mechanical strength. When the sintering temperature was raised to 400 °C, cracks were observed on the fiber surface which were hypothesized to lower mechanical strength (Table 3).

3.2.3. Effects of heating rate

Digital photos of the UFPPMs which were sintered at different heating rates are shown in Fig. 9. When the membranes were sintered at 15 °C/min and 10 °C/min, the nascent fiber membranes severely shrank. This is likely due to the PTFE melting. As the heating rate decreasing, the melt PTFE could easily fill the cavities which were left by the decomposition of PVA. During this process, the fiber shape and the membrane shape maintained.

3.3. Membrane properties

3.3.1. Effect of PTFE/PVA mass ratios

The properties in terms of WCA, porosity, LEP, and mechanical strength of the UFPPMs at different PTFE/PVA mass ratios are listed in Table 2. All of the UFPPMs exhibited excellent hydrophobicity. When the mass ratio of PTFE/PVA increased from 2:1 to 10:1, the WCA increased from 138.2 to 147.6°. This is mainly due to the increase in membrane roughness [18]. As discussed above, the structure of UFPPMs transform from fibrous structure to bead-like structure with the increase of PTFE/PVA mass ratios. This resulted in an increase in membrane roughness. These results agree well with the proposed morphology evolution (Fig. 7a-d).

All of the prepared UFPPMs had high porosities higher than 76%. As the mass ratio of PTFE/PVA increased, a slight decrease in porosity of the resulting material was observed along with a slight increase in mean pore size. This may be a result of the PTFE/PVA fibers becoming more bead-like in nature. When the mass ratio of PTFE/PVA reached 8:1, the obtained UFPPMs were showed to be PTFE resins rather than fibers (Fig. 6d-e). During the sintering process (360 °C), the bead-like structure of the precursor membranes made it more difficult for the PTFE particles to fuse together at the fiber crossover points which prevented the formation of an interconnected fibrous network structure [19,20]. This results in a slightly larger mean pore size.

3.3.2. Effect of sintering temperature

The WCA, OCA, porosity, LEP, and mechanical strength of the UFPPMs prepared at different sintering temperatures are shown in Table 3. When the sintering temperature increased from 340 °C to 380 °C, the PTFE particles began to fuse together at the fiber cross-over points to form an interconnected fibrous network structure. This decreased the mean pore size of the membrane and increased the mechanical strength. Moreover, the pore size distribution of the

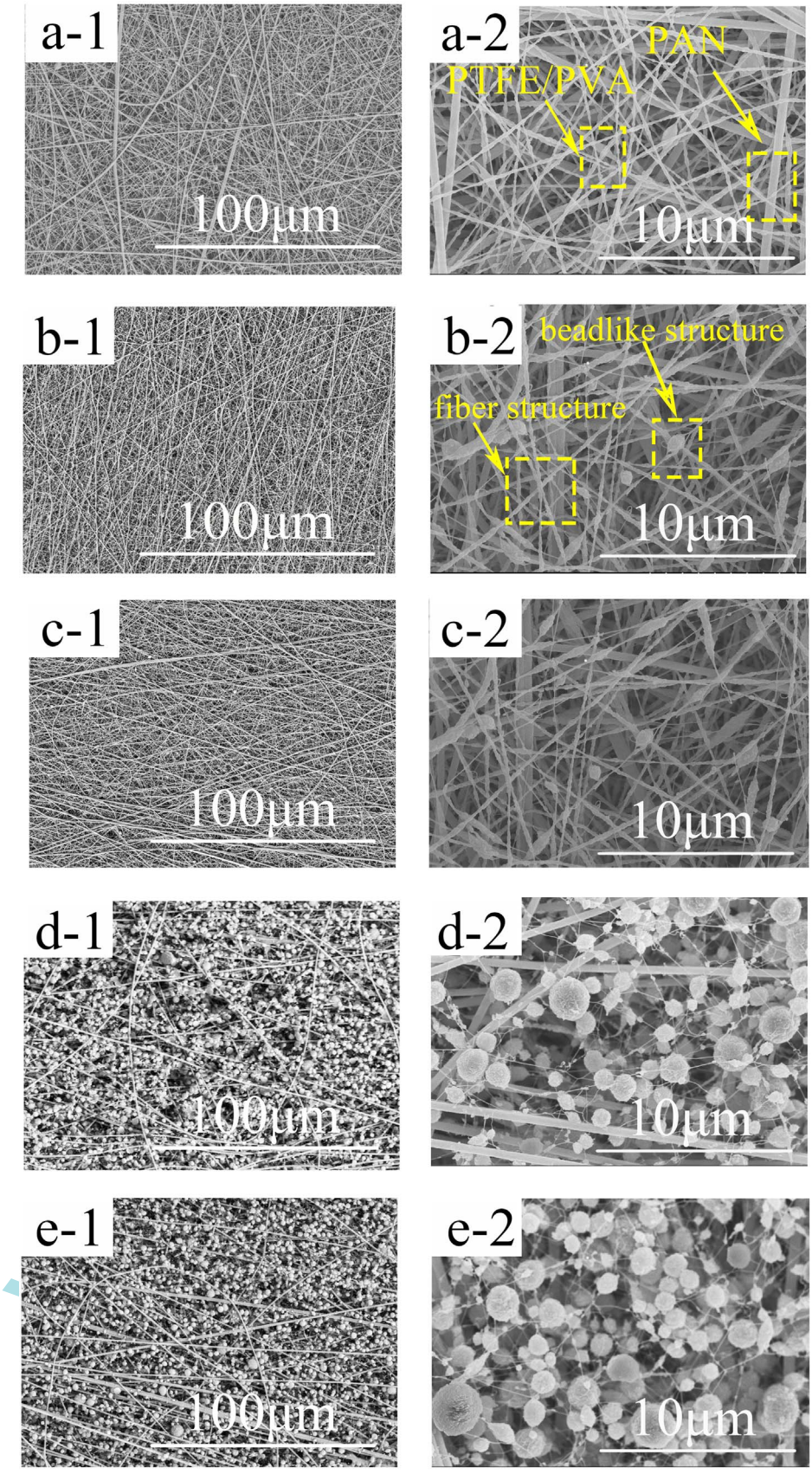

Fig. 6. Morphologies of precursor electrospun PTFE/PVA composite membranes at different PTFE/PVA mass ratios ((a) M-p2, (b) M-p4, (c) M-p6, (d) M-p8, (e) M-p10). The top-right shows digital photos of the UFPPMs..

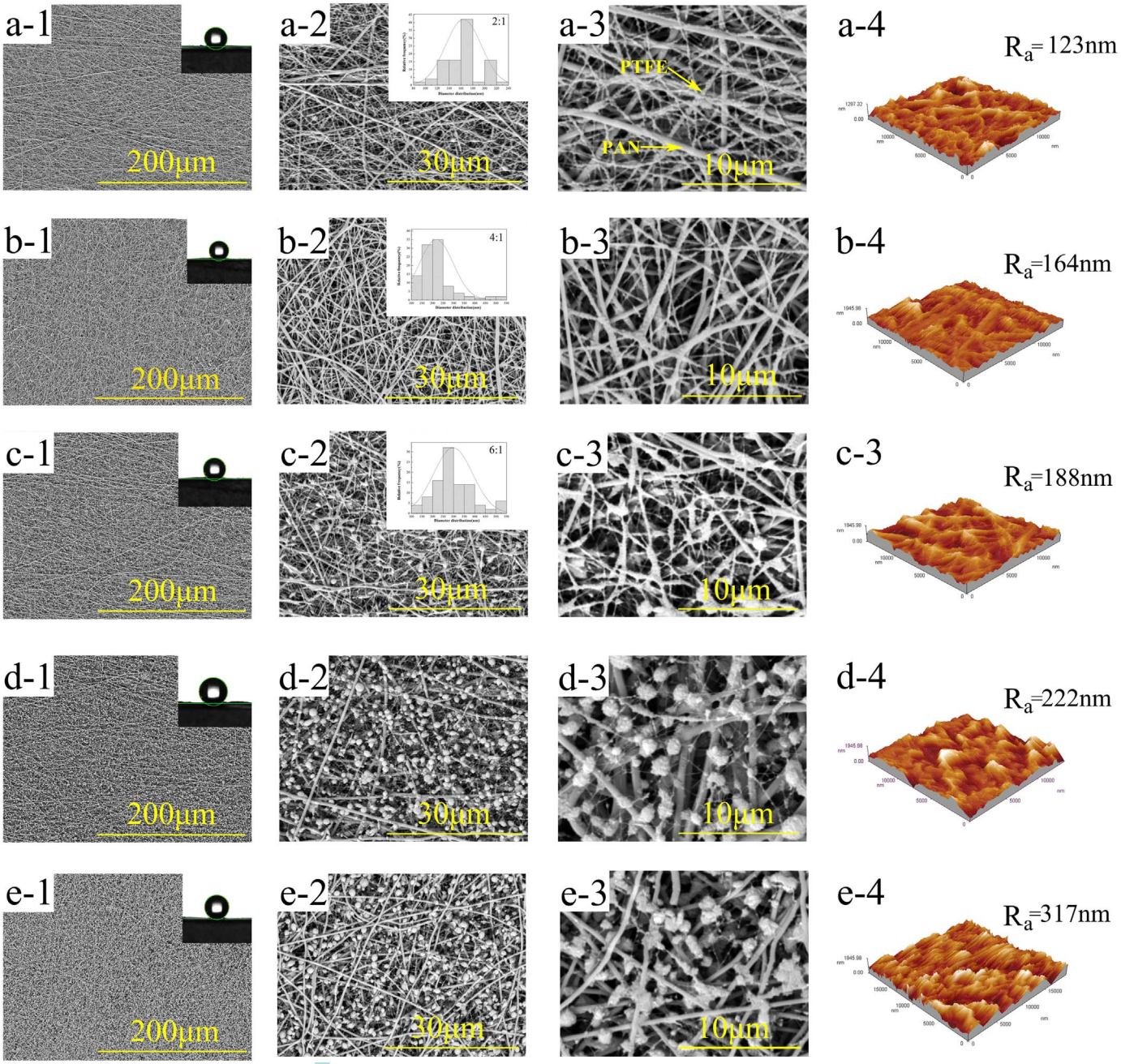

Fig. 7. Morphologies of UFPPMs at different PTFE/PVA mass ratios sintered at 360 °C for (a) M-s2, (b) M-s4, (c) M-s6, (d) M-s8, (e) M-s10 (1:500× surface, 2:3000× surface, 3:8000× surface, 3D AFM images). The top-right corner corresponds to photos of the WCA of each membrane and the diameter distribution of the PTFE ultrafine fibers.

UFPPMs became narrower as sintering temperature was increased (Fig. 10). However, when the sintering temperature was raised to 400 °C, a decrease in mechanical strength was observed along with a wider pore size distribution due to cracks on the PTFE fibers (Fig. 8d-1).

The UFPPMs exhibited strong hydrophobicity and excellent lipophilicity. Changes in the WCA evolution are shown in Fig. 11(a), and the lipophilicity of the UFPPMs are shown in Fig. 11(b). Their affinity for oils and their loose and porous structure were demonstrated by observing the absorption of kerosene. The UFPPMs completely absorbed a droplet of kerosene in 3724 ms, upon which the oil contact angle went to 0 °. This showed that the UFPPMs had very good lipophilicity and would be useful for oil-water separations.

With the similar preparation condition of sintering temperature and PTFE/PVA ratio, the mechanical strength of UFPPMs increased from 0.72 MPa (Table 2) to 4.15 MPa (Table 3). The reason was the increase of membrane's thickness from 29 μm to 126 μm. The increased membrane thickness brought about the increased content of PAN nanofiber, which induced a much higher mechanical strength. The reinforcing mechanism was on the basis of fiber reinforcement and interpenetration between layers. As for fiber reinforcing, during the sintering process, PAN nanofibers formed a stable trapezoidal structure due to the cyclization reaction, which left in the final UFPPMs. The left stable trapezoidal structure of PAN would reinforce the final UFPPMs. As for the interpenetration between layers, the left stable trapezoidal structure of PAN would interpenetrate between the nanofiber layers, which would reinforce the final UFPPMs.

4. VMD test

The UFPPMs were tested for VMD to evaluate their performance for water desalination and especially in harsh water with acid/alkali.

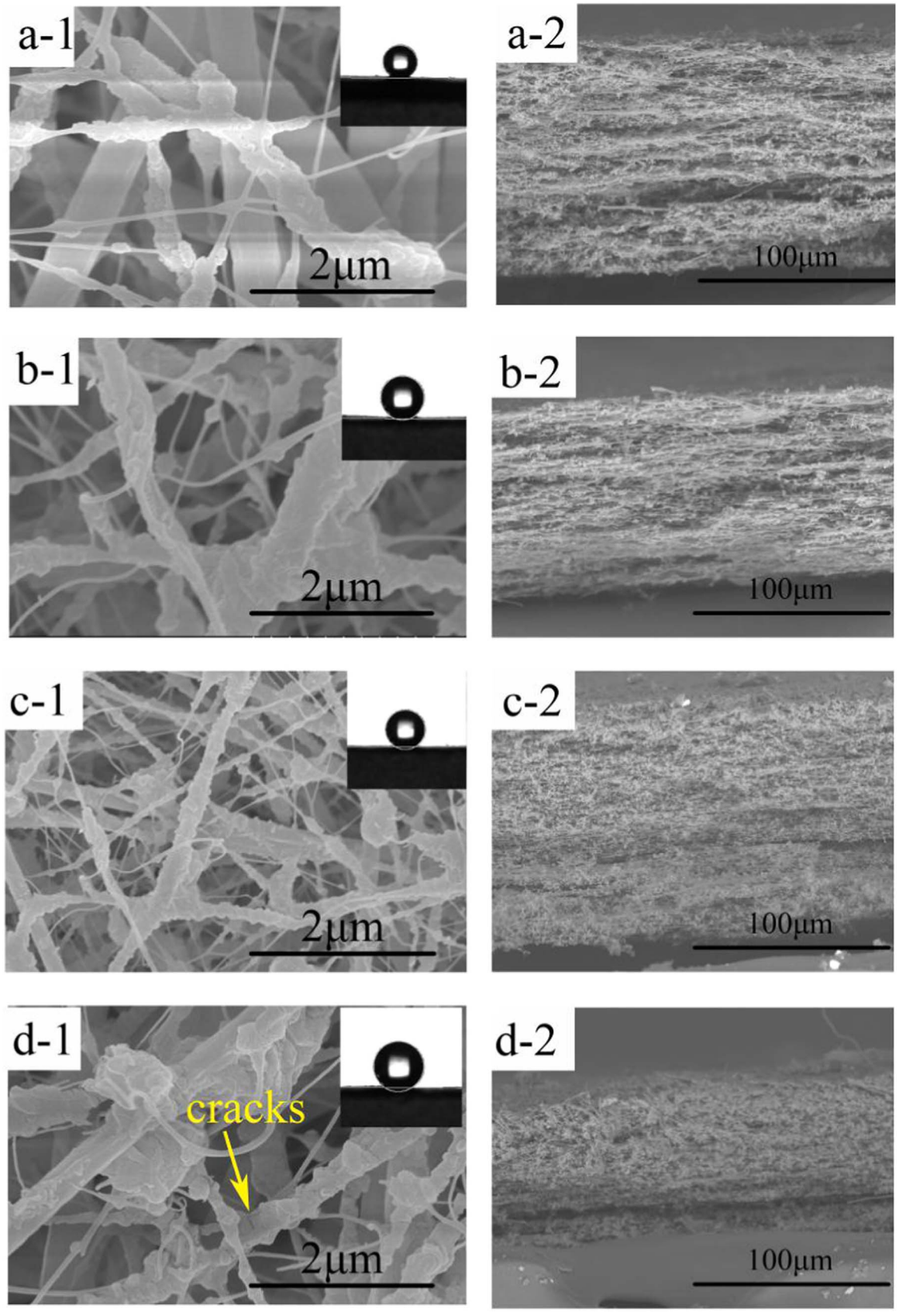

Fig. 8. Morphologies of the UFPPMs sintered at (a) 340 °C, (b) 360 °C, (c) 380 °C, and (d) 400 °C. The top-right corner shows the corresponding photos of the membrane's WCA.

Fig. 9. Digital photos of the UFPPMs prepared using different heating rates of (B) 15 °C/min, (C) 10 °C/min, (D) 5 °C/min, and (E) 1 °C/min. The sintering temperature was 380 °C and the nascent membrane is shown in (A)..

Table 2
The properties of UFPPMs prepared at different PTFE/PVA mass ratios at a sintering temperature of 360 °C.

Samples	Thickness (μm)	Mean diameter of ultrafine fibers (nm)	Porosity (%)	Mean pore size (μm)	WCA (°)	LEP (MPa)	Mechanical strength (MPa)
M-s2	25 ± 4.0	164.2	85.4 ± 3.5	0.68 ± 0.10	138.2 ± 2.3	—	—
M-s4	21 ± 2.0	212.2	86.2 ± 2.7	0.81 ± 0.04	143.3 ± 1.8	0.06 ± 0.01	0.50 ± 0.08
M-s6	29 ± 2.0	297.3	81.1 ± 4.2	0.79 ± 0.06	143.6 ± 2.4	0.11 ± 0.02	0.72 ± 0.20
M-s8	24 ± 2.0	—	79.5 ± 4.4	0.97 ± 0.12	145.2 ± 3.2	0.10 ± 0.01	0.69 ± 0.07
M-s10	32 ± 4.0	—	76.3 ± 5.0	1.16 ± 0.10	147.6 ± 1.8	0.08 ± 0.02	0.53 ± 0.12

Table 3
The properties of UFPPMs prepared at different sintering temperatures (PTFE/PVA mass ratio was 6:1).

Sintering temperature (°C)	Thickness (μm)	Porosity (%)	Max pore size (μm)	Mean pore size (μm)	WCA (°)	Kerosene contact angle (°)	LEP (MPa)	Mechanical strength (MPa)	Elongation at break (%)	Young's modulus (MPa)
340	132 ± 6	78.5 ± 5.4	0.93	0.83 ± 0.10	143.4 ± 1.8	21.4 ± 1.9	0.19 ± 0.02	3.25 ± 0.12	7.8 ± 1.8	41.67 ± 6.6
360	127 ± 4	84.2 ± 4.2	0.78	0.76 ± 0.02	146.6 ± 2.0	22.2 ± 1.6	0.21 ± 0.01	4.15 ± 0.14	10.6 ± 1.6	39.15 ± 3.9
380	126 ± 2	86.3 ± 3.4	0.86	0.75 ± 0.11	156.6 ± 1.7	21.9 ± 2.0	0.21 ± 0.01	4.17 ± 0.08	10.5 ± 0.8	39.71 ± 2.1
400	118 ± 2	86.0 ± 3.9	0.69	0.65 ± 0.04	159.3 ± 1.7	16.8 ± 1.8	0.16 ± 0.02	2.76 ± 0.10	7.50 ± 1.9	36.80 ± 6.4

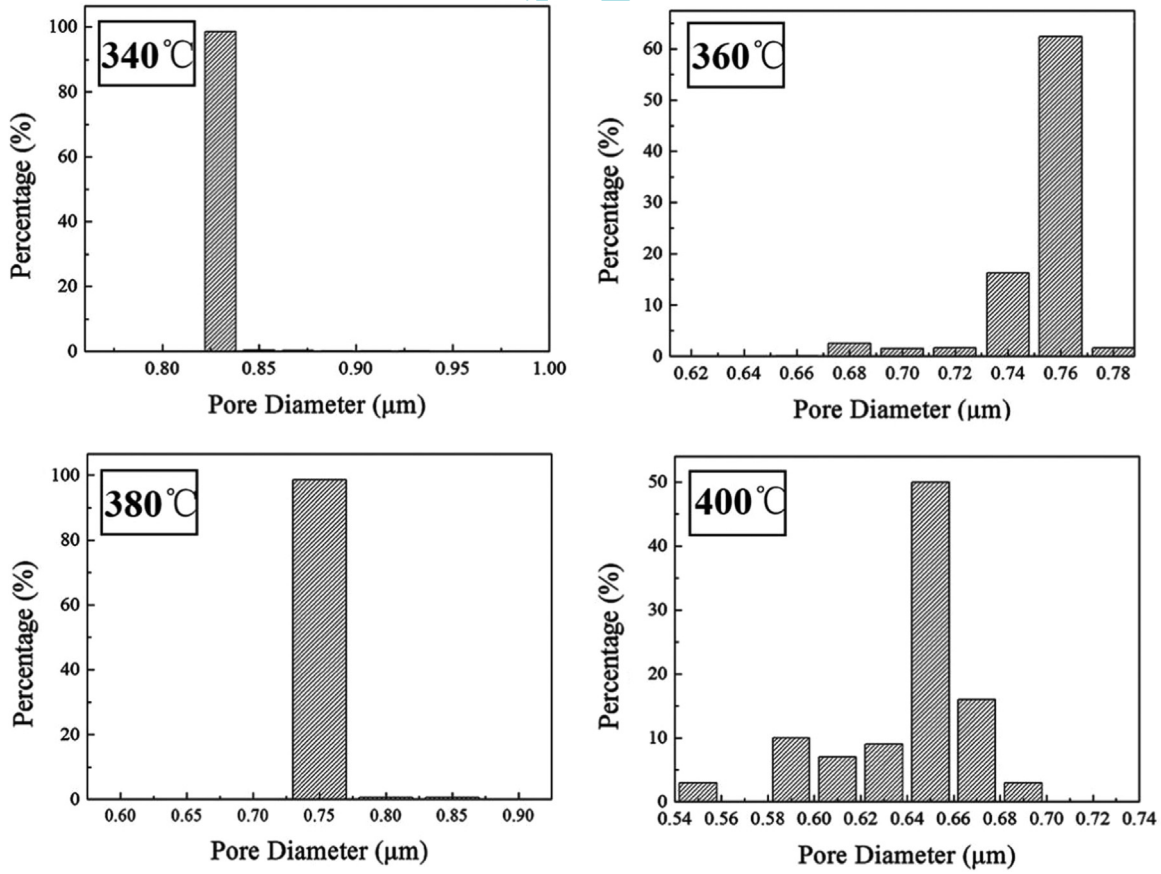

Fig. 10. Pore size distributions of UFPPMs prepared at different sintering temperatures (PTFE/PVA mass ratio: 6:1).

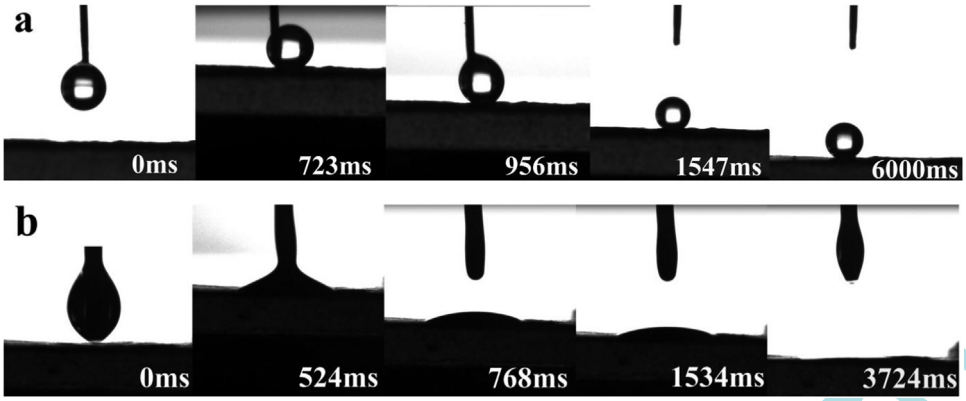

Fig. 11. Images of contact angle measurements, showing (a) the WCA and the (b) OCA drop evolution (a FTFE/PVA mass ratio of 6:1 and a sintering temperature of 380 °C).

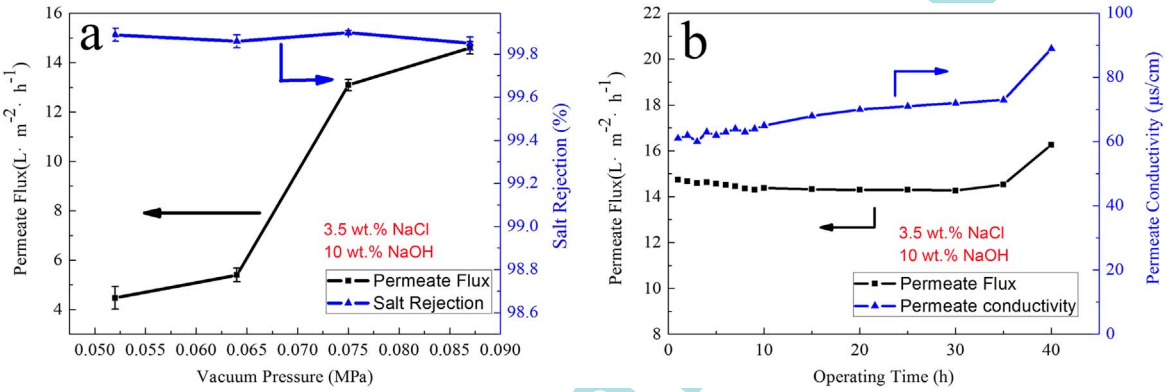

Fig. 12. Effects of (a) vacuum pressure and (b) operating time on the permeate flux and permeate conductivity (80 °C feed temperature, 1.5 L/min diaphragm pump flow rate, 0.08 MPa vacuum pressure).

The results of the permeate flux and the salt rejection are shown in Fig. 12.

As shown in Fig. 12a, increasing the vacuum can effectively improve the permeate flux. The salt rejections remained above 99.8% and the permeate flux was as high as 14.59 L m^{-2}·h^{-1} with a vacuum pressure of 0.087 MPa.

The long term stability of the UFPPMs was also evaluated over a MD operation with the mixed aqueous solution of 3.5 wt% NaCl and 10 wt% NaOH as the saline feed solution. As shown in Fig. 12b, after operating for 35 h, the permeate conductivity and permeate flux were stable without any obvious decrease, and the salt rejection remained above 99.8%. Compared with other published MD processes [21–23], the UFPPMs exhibit a great potential and feasibility for their use in MD process for harsh water treatment.

5. Conclusions

The UFPPMs were fabricated by controlling the PTFE/PVA mass ratio, the sintering temperature, and the heating rate. The best performing UFPPM was made from a PTFE/PVA mass ratio of 6:1 and sintered at 380 °C. The UFPPMs produced from these conditions demonstrated super-hydrophobicity and excellent lipophilicity, and performed well in harsh water desalination. In VMD, the permeate flux stabilized at 14.53 L m^{-2} h^{-1}, and the salt rejections were maintained above 99.8% after operating for 35 h. The long-term operation of the UFPPM in VMD indicates that they have excellent stability in harsh water desalination experiments.

Acknowledgments

This work was supported by the National Natural Science Foundation of China (No. 21404079), the National Basic Research Program of China (2014CB660813), and the Specialized Research Fund for the Doctoral Program of Higher Education (20131201120003).

Appendix A.

Symbol	Definition
ε	porosity (%)
W_1	weight of the wet membrane (g)
W_2	the weight of the dry membrane(g)
ρ	the density (g/ml)
d	the average thickness of the membrane(mm)

J	oil permeation flux ($L \cdot m^{-2} \cdot h^{-1}$),
V	the volume of the permeated oil (L),
A	membrane area (m^2)
R	rejection (%)
C_f	concentration of the ink in the feed
C_p	concentration of the permeate solution

References

[1] Z.M. Huang, Y.Z. Zhang, M. Kotaki, et al., A review on polymer nanofibers by electrospinning and their applications in nanocomposites, Compos. Sci. Technol. 63 (15) (2003) 2223–2253.

[2] S. Simone, A. Figoli, A. Criscuoli, et al., Preparation of hollow fibre membranes from PVDF/PVP blends and their application in VMD, J. Membr. Sci. 364 (1) (2010) 219–232.

[3] K.W. Lawson, D.R. Lloyd, Membrane distillation, J. Membr. Sci. 124 (1) (1997) 1–25.

[4] M. Spasova, R. Mincheva, D. Paneva, et al., Perspectives on: criteria for complex evaluation of the morphology and alignment of electrospun polymer nanofibers, J. Bioact. Compat. Polym. 21 (5) (2006) 465–479.

[5] R. Gopal, S. Kaur, C.Y. Feng, et al., Electrospun nanofibrous polysulfone membranes as pre-filters: particulate removal, J. Membr. Sci. 289 (1) (2007) 210–219.

[6] J.A. Prince, G. Singh, D. Rana, et al., Preparation and characterization of highly hydrophobic poly (vinylidene fluoride)–clay nanocomposite nanofiber membranes (PVDF–clay NNMs) for desalination using direct contact membrane distillation[J], J. Membr. Sci. 397 (2012) 80–86.

[7] H. Zhu, H. Wang, F. Wang, et al., Preparation and properties of PTFE hollow fiber membranes for desalination through vacuum membrane distillation, J. Membr. Sci. 446 (2013) 145–153.

[8] Q. Huang, C. Xiao, X. Hu, et al., Study on the effects and properties of hydrophobic poly (tetrafluoroethylene) membrane, Desalination 277 (1) (2011) 187–192.

[9] D.J. Arthur, G.S. Swei. US Patent 5,149, 1992, 590

[10] Guo Y-H (2006) A method to produce PTFE fiber CN1962971A

[11] J. Xiong, P. Huo, F.K. Ko, Fabrication of ultrafine fibrous polytetrafluoroethylene porous membranes by electrospinning, J. Mater. Res. 24 (09) (2009) 2755–2761.

[12] H. Matsuyama, M. Teramoto, S. Kudari, et al., Effect of diluents on membrane formation via thermally induced phase separation, J. Appl. Polym. Sci. 82 (1) (2001) 169–177.

[13] A. Gugliuzza, E. Drioli, PVDF and HYFLON AD membranes: ideal interfaces for contactor applications, J. Membr. Sci. 300 (1) (2007) 51–62.

[14] T. Zhou, Y. Yao, R. Xiang, et al., Formation and characterization of polytetrafluoroethylene nanofiber membranes for vacuum membrane distillation, J. Membr. Sci. 453 (2014) 402–408.

[15] T. Dürrschmidt, H. Hoffmann, Film-forming process from globular polytetrafluoroethylene latex particles, J. Appl. Polym. Sci. 92 (2) (2004) 733–742.

[16] Q.L. Huang, C. Xiao, X. Feng, et al., Design of super-hydrophobic microporous polytetrafluoroethylene membranes, New J. Chem. 37 (2) (2013) 373–379.

[17] Y. Takagi, J.C. Lee, S. Yagi, et al., Fiber making directly from poly (tetrafluoroethylene) emulsion, Polymer 52 (18) (2011) 4099–4105.

[18] A. Marmur, Wetting on hydrophobic rough surfaces: to be heterogeneous or not to be?, Langmuir 19 (20) (2003) 8343–8348.

[19] C.W. Nan, R. Birringer, D.R. Clarke, et al., Effective thermal conductivity of particulate composites with interfacial thermal resistance, J. Appl. Phys. 81 (10) (1997) 6692–6699.

[20] Y.C. Chen, C.C. Tsai, Y.D. Lee, Preparation and properties of silylated PTFE/SiO_2 organic–inorganic hybrids via sol–gel process, J. Polym. Sci. Part A: Polym. Chem. 42 (7) (2004) 1789–1807.

[21] S. Bandini, G.C. Sarti, Concentration of must through vacuum membrane distillation, Desalination 149 (1) (2002) 253–259.

[22] C.K. Chiam, R. Sarbatly, Vacuum membrane distillation processes for aqueous solution treatment–a review, Chem. Eng. Process. Process Intensif. 74 (8) (2013) 27–54.

[23] H. Fan, Y. Peng, Z. Li, et al., Preparation and characterization of hydrophobic PVDF membranes by vapor-induced phase separation and application in vacuum membrane distillation, J. Polym. Res. 20 (6) (2013) 1–15.